Received: 22 August 2024 | Revised: 29 October 2024 | Accepted: 5 November 2024

DOI: 10.1002/kin.21769

INTERNATIONAL JOURNAL OF CHEMICAL KINETICS WILEY

RESEARCH ARTICLE

Rate coefficients for the gas-phase reaction of OH radicals with the L_4, L_5, D_5, and D_6 permethylsiloxanes

François Bernard[1,2] | **James B. Burkholder**[1]

[1]Chemical Sciences Laboratory, National Oceanic and Atmospheric Administration, Boulder, Colorado, USA

[2]Cooperative Institute for Research in Environmental Sciences, University of Colorado, Boulder, Colorado, USA

Correspondence
James B. Burkholder, Chemical Sciences Laboratory, National Oceanic and Atmospheric Administration, Boulder, CO 80305, USA.
Email: James.B.Burkholder@noaa.gov

Present address
François Bernard, Independent Research Scientist, Orléans, France

Abstract

Rate coefficients, k(T), for the gas-phase OH radical reaction with decamethyltetrasiloxane ($(CH_3)_3SiO[Si(CH_3)_2O]_2Si(CH_3)_3$, L_4, k_1), dodecamethylpentasiloxane ($(CH_3)_3SiO[Si(CH_3)_2O]_3Si(CH_3)_3$, L_5, k_2), and decamethylcyclopentasiloxane ($[-Si(CH_3)_2O-]_5$, D_5, k_3), and dodecamethylcyclohexasiloxane ($[-Si(CH_3)_2O-]_6$, D_6, k_4) were measured using a pulsed laser photolysis—laser induced fluorescence absolute method over the temperature range 270–370 K. The obtained room temperature rate coefficients, with quoted 2σ absolute uncertainties, and fitted temperature dependence are (cm^{-3} $molecule^{-1}$ s^{-1}):

$$k_1\,(295\text{ K}) = (2.50 \pm 0.18) \times 10^{-12}, \quad k_1\,(270-370\text{ K}) = 1.707 \times 10^{-13}(\text{T}/298)^{4.45} \exp(807/\text{T})$$

$$k_2\,(295\text{ K}) = (3.12 \pm 0.32) \times 10^{-12}, \quad k_2\,(295-370\text{ K}) = (2.65 \pm 0.02) \times 10^{-11} \exp(-(630 \pm 60)/\text{T})$$

$$k_3\,(295\text{ K}) = (2.02 \pm 0.12) \times 10^{-12}, \quad k_3\,(270-370\text{ K}) = 8.97 \times 10^{-13}(T/298)^{2.90} \exp(248/\text{T})$$

$$k_4\,(297\text{ K}) = (2.89 \pm 0.16) \times 10^{-12}, \quad k_4\,(297-370\text{ K}) = (3.13 \pm 0.05) \times 10^{-11} \exp(-(717 \pm 119)/\text{T})$$

The 2σ absolute rate coefficient uncertainty, for all compounds included in this study, is conservatively estimated to be ~10% over the entire temperature range. The cyclic permethylsiloxanes were found to be less reactive than the analogous linear compound, while both linear and cyclic compounds show increasing reactivity with increasing number of CH_3- groups. A structure activity relationship (SAR) parameterization for the permethylsiloxanes is presented. The estimated atmospheric lifetimes due to OH reaction for L_4, L_5, D_5, and D_6 are 5.2, 4.4, 6.8, and 5.2 days, respectively.

KEYWORDS
D_5, D_6, L_4, L_5, OH radicals, permethylsiloxanes

1 | INTRODUCTION

Permethysiloxanes are man-made organosilicon compounds consisting of alternating silicon and oxygen atoms with methyl groups attached to the silicon atoms. Permethylsiloxanes are volatile chemical products (VCPs)[1] that are used in a variety of applications and products, for example, personal care products, lubricants, and cleaning agents. Permethylsiloxanes are emitted into the atmosphere during production and use and have been observed in a variety of urban,[2–5] indoor,[6–10] and remote[11–14] environments. The impact and atmospheric modeling[15–17] of permethylsiloxanes on air quality, in particular, through particle nucleation[18,19] and the formation of secondary organic aerosol (SOA)[20–24] is an active area of environmental research in addition to concerns of terrestrial- and bio-accumulation, for example, see Zhang et al.[25]

A predominant atmospheric (gas-phase) loss process for permethylsiloxanes is by reaction with the OH radical. Rate coefficients, k, for the OH radical reaction with the linear L_4 and L_5 and cyclic D_5 and D_6 permethylsiloxanes (see Figure 1):

$$OH + (CH_3)_3SiO\left[(CH_3)_2SiO\right]_2Si(CH_3)_3 \rightarrow \text{Products} \quad L_4 \quad (1)$$

$$OH + (CH_3)_3SiO\left[(CH_3)_2SiO\right]_3Si(CH_3)_3 \rightarrow \text{Products} \quad L_5 \quad (2)$$

$$OH + \left[-Si(CH_3)_2O-\right]_5 \rightarrow \text{Products} \quad D_5 \quad (3)$$

$$OH + \left[-Si(CH_3)_2O-\right]_6 \rightarrow \text{Products} \quad D_6 \quad (4)$$

were measured in this study. The reaction proceeds via H-atom abstraction from a methyl group. The linear permethylsiloxanes contain both terminal and internal methyl groups, while for the cyclic permethylsiloxanes all the methyl groups are identical.

There are several relative rate kinetic studies in the literature that have reported rate coefficient data for reactions 1–4 using various techniques to monitor the loss of the permethylsiloxane and a reference compound.[26–30] The reported $k_{1\text{-}4}$(297 K) values fall in the range between 1.55×10^{-12} cm^{-3} molecule^{-1} s^{-1} for D_5 and 3.4×10^{-12} cm^{-3} molecule^{-1} s^{-1} for L_5. The only temperature-dependent rate coefficient data was reported by Safron et al. and Xiao et al. for the D_5[29,30] and D_6[30] reactions at temperatures between 313 and 353 K. Results from previous studies are discussed in the Section 3.

In this study, rate coefficients for reactions 1–4 in the gas-phase were measured over the temperature range 270–370 K using a pulse laser photolysis—laser induced fluorescence (PLP–LIF) absolute measurement technique. This study is an extension of our previous study of the rate coefficient temperature dependence for the OH radical reaction with the permethylsiloxanes L_2, L_3, D_3, and D_4.[31] The results from our study provide a temperature-dependent update to the room temperature rate coefficient OH + permethylsiloxane structure activity relationship (SAR) provided by Alton and Browne.[26]

2 | EXPERIMENTAL DETAILS

Rate coefficients, k(T), for reactions 1–4 were measured using a pulsed laser photolysis (PLP)—laser induced

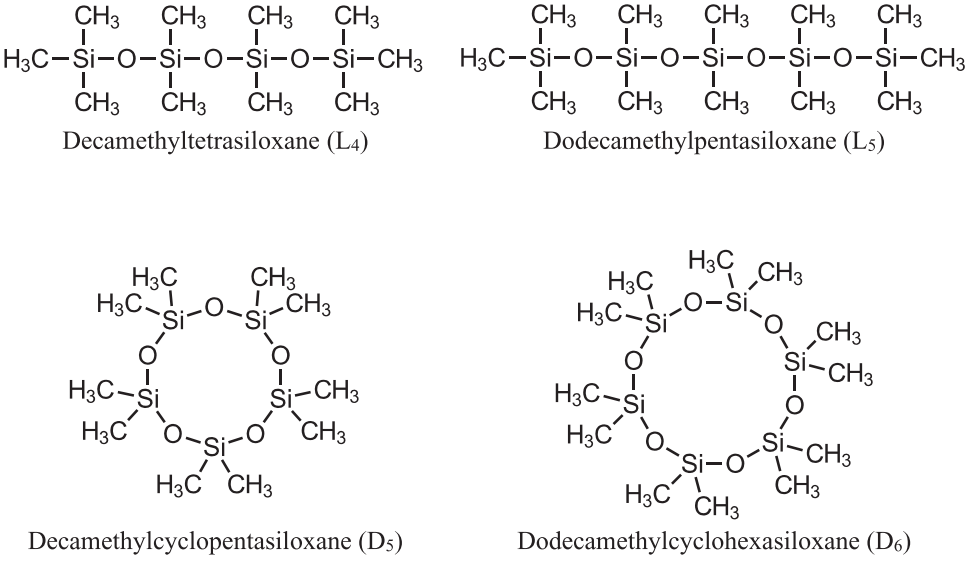

FIGURE 1 Permethylsiloxanes were included in this study.

fluorescence (LIF) technique. Measurements were performed over a range of temperature, 270–370 K, and pressure, 50–200 Torr (He bath gas). No pressure dependence was observed over this range of conditions. The experimental apparatus used in this study has been used in previous studies[32,33] from this laboratory and only a brief description is given here.

The pulsed photolysis and probe beams passed through a jacketed multi-port Pyrex LIF reactor (150 cm^{-3} internal volume) at right angles and intersected in the middle of the reactor. OH fluorescence was detected orthogonally to the photolysis and probe beams. The temperature in the reactor was maintained by circulating fluid from a temperature-regulated reservoir through the LIF reactor jacket. The temperature of the gas in the reaction zone was measured with a retractable thermocouple to an accuracy of 0.5 K.

Rate coefficients were measured under pseudo-first-order conditions in OH, that is, [Permethylsiloxanes] > > [OH]. OH radicals were produced by 248 nm pulsed laser photolysis (KrF excimer laser) of H_2O_2, HNO_3, or $(CH_3)_3COOH$:

$$H_2O_2 + h\nu \rightarrow 2OH \quad (5)$$

$$HNO_3 + h\nu \rightarrow OH + NO_2 \quad (6)$$

$$(CH_3)_3COOH + h\nu \rightarrow OH + \text{Products} \quad (7)$$

H_2O_2 was the primary OH radical precursor used in this study, while $(CH_3)_3COOH$ was used in measurements at 295 and 320 K, and HNO_3 was used in several measurements at temperatures ≥295 K.

OH radical fluorescence was probed by exciting the $A^2\sum^+ (v' = 1) \leftarrow X^2\prod (v'' = 0)$ transition at 282 nm using a frequency doubled Nd:YAG pumped dye laser operating at 10 Hz. The OH fluorescence was detected by a photomultiplier tube (PMT) mounted orthogonal to the photolysis and probe laser beams. OH fluorescence was collected using a pair of convex lenses and passed through a 308 nm band pass filter (full width at half maximum (FWHM) of ~10 nm) mounted in the front of the PMT. The PMT signal was averaged for 100 laser shots with a gated charge integrator. OH temporal profiles were obtained by varying the delay between the photolysis and probe lasers between 10 μs and 20 ms.

The initial OH radical concentration, $[OH]_0$, was estimated from:

$$[OH]_0 = \sigma(248\ \text{nm})\phi(248\ \text{nm})\,F\,[\text{Precursor}] \quad (8)$$

where σ(248 nm) is the absorption cross-section of the precursor at 248 nm and ϕ(248 nm) is the precursor OH quantum yield. The photolysis laser fluence, F, was measured at the entrance and exit of the LIF reactor using a power meter. The photolysis fluence was varied over the range 0.5–2.6 mJ cm^{-2} $pulse^{-1}$ in this study. The precursor concentration was estimated from the pseudo-first-order decay of OH radicals in the absence of the permethylsiloxane. Precursor concentrations were in the range $(0.41–30) \times 10^{14}$ molecule cm^{-3}. Rate coefficients, absorption cross sections, and quantum yields were taken from Burkholder et al.[34] for H_2O_2 and HNO_3 and from Baasandorj et al.[35] for $(CH_3)_3COOH$. For the conditions used in our experiments, $[OH]_0$ was in the range $(0.51–12.3) \times 10^{10}$ molecule cm^{-3}.

OH radical temporal profiles were described by the integrated rate equation:

$$\ln\left(\frac{[OH]_t}{[OH]_0}\right) = \ln\left(\frac{S_t}{S_0}\right) = -(k\,[\text{Permethylsiloxane}] + k_d)\,t = -k't \quad (9)$$

where S_t and S_0 are the measured OH fluorescence signal at times t and t_0, which are proportional to $[OH]_t$ and $[OH]_0$, respectively. k' and k_d are the pseudo first-order rate coefficients in the presence and absence of permethylsiloxanes, respectively. k_d is the OH radical removal by reaction with the precursor and diffusion out of the detection volume. k_d values ranged from 64 to 665 s^{-1} depending on the experimental conditions and precursor concentration. k' was obtained from a weighted linear least-squares analysis of the OH temporal profiles. k' was measured at different concentrations of permethylsiloxanes for a range of temperatures. Measured k' values ranged from 138 to 2604 s^{-1}. The bimolecular rate coefficient, k(T), was obtained from an unweighted linear least-squares fit of k' versus [permethylsiloxane].

Online infrared absorption measurements were used to determine the concentration of permethylsiloxanes in the LIF reactor. Infrared measurements were made after the gases passed through the LIF reactor. Infrared spectra of permethylsiloxanes were recorded using a Fourier transform infrared spectrometer equipped with a multi-pass absorption cell (485 cm path-length) with KBr windows. The infrared spectra were recorded by co-adding 100 interferograms at a spectral resolution of 1 cm^{-1}. Permethylsiloxane infrared band strengths used in this work were taken from a previous study in this laboratory.[36] The infrared spectra used to quantify the permethylsiloxane concentrations have estimated uncertainties of 5%, or less.

Materials. The purity of the decamethyltetrasiloxane (L_4), dodecamethylpentasiloxane (L_5), and decamethylcyclopentasiloxane (D_5) samples was reported by the supplier to be 97%. The purity of dodecamethylcyclohexasiloxane (D_6) was reported to be >98.0%. These compounds

have fairly low-volatility and for reference, the room temperature vapor pressure of the compounds are approximately 0.3, 0.08, 0.15, and 0.02 Torr for L_4, L_5, D_5, and D_6, respectively, as estimated in this work. The samples were degassed in several freeze (77 K)-pump-thaw cycles and stored under vacuum in Pyrex reservoirs. The permethylsiloxanes were introduced into the vacuum system by passing a flow of He carrier gas through a reservoir containing the pure sample. On the basis of an infrared spectrum analysis, the D_5 sample contained a minor L_2 impurity and the D_6 sample contained minor L_2 and D_3 impurities. There were no infrared detectable impurities in the L_4 and L_5 samples. Kinetic measurements performed over the course of the study, using the same sample, agreed to within the measurement precision, which suggests an absence of volatile reactive impurities in the samples.

He (UHP, 99.999%) and O_2 (UHP, 99.99%) were used as supplied. H_2O_2, $(CH_3)_3COOH$, and HNO_3 were prepared and used as described previously.[37] Gas flows were measured using calibrated electronic flow meters and pressures were measured using capacitance manometers. Quoted uncertainties are 2σ (95% confidence level) unless stated otherwise.

3 | RESULTS AND DISCUSSION

The experimental conditions and rate coefficients obtained in this study for reactions 1–4 are given in Tables 1–4, respectively. The measured OH temporal profiles for each of the permethylsiloxanes obeyed first-order kinetics, that is, single exponential decays, for all experimental conditions included in this study. Representative OH temporal profiles are provided in Figure S1. Note that the low-temperature rate coefficient experiments needed to take into consideration the vapor pressure of the permethylsiloxane to avoid condensation of the sample in the apparatus. The low-temperature measurements, therefore, had a smaller range of measured k' values. The results for the linear and cyclic permethylsiloxanes are presented separately below.

3.1 | Linear permethylsiloxanes, L_4 and L_5

The pseudo-first-order rate coefficient data obtained for reaction 1 at 270, 295, and 370 K is shown in Figure 2. Data obtained at all temperatures is given in Figure S2. The pseudo-first-order rate coefficient data for reaction 2 is of similar quality and is shown in Figure S3. Both reactions showed no dependence on variations in the experimental conditions, for example, radical precursor and $[OH]_0$, as outlined in Tables 1 and 2. The final derived rate coefficient at each temperature was obtained from a fit of the combined data obtained at each temperature.

The temperature dependent rate coefficient results for reactions 1 and 2 are summarized in Figures 3 and 4, respectively. Reactions 1 and 2 show a positive temperature dependence. The L_4 reaction displays a weak non-Arrhenius behavior, while over the more limited temperature range of the L_5 reaction measurements an Arrhenius behavior reproduces the data very well, to within the estimated measurement uncertainty of ~10%. The temperature dependence fit results are given in Table 5.

3.2 | Comparison with previous L_4 and L_5 studies

The previous room temperature studies of Reactions 1 and 2 are included in Table 5 and Figures 3 and 4 for comparison with the present results. Markgraf and Wells[28] performed a relative rate study, with *n*-hexane and cyclohexane reference reactions and reported $k_1(297\ K) = (2.66 \pm 0.13) \times 10^{-12}$ cm^{-3} molecule^{-1} s^{-1} (the quoted uncertainty represents the measurement precision; we estimate that the absolute uncertainty would be ~0.3, 1σ). Note that the currently recommended rate coefficient for the cyclohexane rate coefficient, see Table 5 footnote, is ~7% greater than that used in the Markgraf and Wells study. However, it appears that the Markgraf and Wells result was primarily based on the *n*-hexane results. Their result is slightly greater than the present results, but the agreement is within the combined uncertainty estimates. Alton and Browne[26] used an environmental chamber relative rate method with chemical ionization mass spectrometry detection and propionic acid and methyl ethyl ketone reference compounds. In their final analysis, the L_2 absolute rate coefficient from the Bernard et al.[31] study was used to provide an intra-siloxane relative rate determination. Their reported L_4 $k_1(297\ K)$ value is identical to our room temperature value. Alton and Browne[26] reported a value for L_5 of $k_2(297\ K) = (3.4 \pm 0.5) \times 10^{-12}$ cm^{-3} molecule^{-1} s^{-1} that is also in good agreement with our room temperature result. The 1σ measurement precision uncertainty reported in the Alton and Browne[26] study is similar, or slightly greater, than the 2σ absolute uncertainty in our recommended $k_1(295\ K)$ and $k_2(295\ K)$ values.

3.3 | Cyclic permethylsiloxanes, D_5 and D_6

The pseudo-first-order rate coefficient data obtained for Reactions 3 and 4 are shown graphically in Figures S4

TABLE 1 Summary of the experimental conditions and rate coefficients, k_1(T), obtained in this work for the OH + decamethyltetrasiloxane (L_4) reaction.

T (K)	P (Torr)	v (cm s^{-1})	OH radical source	[Source] (10^{14} molecule cm^{-3})	Photolysis laser Fluence (mJ cm^{-2} $pulse^{-1}$)	$[OH]_0$ (10^{10} molecule cm^{-3})	$[L_4]$ (10^{14} molecule cm^{-3})	k(T)[a] (10^{-12} cm^{-3} $molecule^{-1}$ s^{-1})
370	100	16.2	H_2O_2	0.9	2.1	4.3	0.67–4.73	3.99 ± 0.09
370	50	32.6	H_2O_2	1.7	2.0	7.8	0.56–4.14	4.13 ± 0.07
370	250	14.0	H_2O_2	0.4	1.8	1.7	0.55–2.46	4.05 ± 0.12
370	100	16.0	HNO_3	20.9	1.6	8.2	0.69–5.38	3.79 ± 0.10
371	100	24.4	H_2O_2	1.2	1.9	5.0	0.38–4.87	3.97 ± 0.10
370	100	16.2	HNO_3	23.5	1.4	8.1	0.77–4.99	3.93 ± 0.12
370	100	16.8	HNO_3	22.3	1.5	8.2	0.72–4.61	3.91 ± 0.14
								Global fit: k(370 K) = 3.94 ± 0.03
340	100	14.8	H_2O_2	1.2	2.3	6.0	0.68–6.52	3.43 ± 0.06
340	100	15.1	H_2O_2	1.4	1.5	4.9	0.59–6.65	3.36 ± 0.05
340	200	7.5	H_2O_2	1.5	1.6	5.7	1.21–5.66	3.37 ± 0.06
								Global fit: k(340 K) = 3.39 ± 0.02
320	100	13.9	H_2O_2	1.0	2.4	5.1	0.61–7.21	2.94 ± 0.05
320	100	13.8	HNO_3	30.0	1.6	12.3	0.81–4.96	2.75 ± 0.13
320	200	6.9	H_2O_2	1.6	1.6	5.8	0.95–6.22	2.99 ± 0.12
320	50	28.2	H_2O_2	2.3	1.6	8.2	1.27–7.33	2.97 ± 0.06
320	100	14.1	H_2O_2	1.4	1.4	4.3	1.12–5.93	2.97 ± 0.05
320	100	13.7	$(CH_3)_3COOH$	1.4	1.5	0.5	0.67–7.01	2.80 ± 0.08
320	100	14.0	HNO_3	20.3	1.4	6.9	1.17–5.93	2.88 ± 0.07
								Global fit: k(320 K) = 2.90 ± 0.03
295	99	12.7	H_2O_2	0.8	2.5	4.5	1.66–6.56	2.51 ± 0.10
295	101	26.1	H_2O_2	0.9	2.1	4.2	0.87–4.31	2.39 ± 0.04
295	200	6.5	H_2O_2	1.0	1.8	4.1	0.83–7.23	2.58 ± 0.07
295	100	13.1	H_2O_2	1.3	2.5	7.3	1.13–6.50	2.50 ± 0.07
295	100	13.0	H_2O_2	0.9	2.6	5.4	0.71–5.77	2.56 ± 0.06[b]
295	50	14.3	H_2O_2	1.9	1.4	6.0	0.84–8.88	2.54 ± 0.03
295	50	26.2	H_2O_2	1.8	2.0	7.9	0.65–7.80	2.47 ± 0.04
295	50	30.9	H_2O_2	1.7	1.7	6.5	0.34–5.78	2.56 ± 0.06
295	100	12.8	H_2O_2	1.6	1.3	4.8	1.32–7.25	2.44 ± 0.06
295	200	6.4	H_2O_2	1.6	1.3	4.7	0.91–5.47	2.54 ± 0.04
295	100	12.9	H_2O_2	1.7	1.0	3.7	0.91–6.66	2.52 ± 0.05
295	61	20.3	H_2O_2	2.1	2.1	10.0	0.81–6.06	2.57 ± 0.07
295	50	26.1	H_2O_2	1.4	2.0	6.6	0.69–6.44	2.53 ± 0.04
294	100	12.9	HNO_3	23.6	1.9	11.1	1.12–7.19	2.38 ± 0.05
295	50	25.6	HNO_3	15.2	1.8	7.0	0.98–6.35	2.46 ± 0.06
295	100	12.7	$(CH_3)_3COOH$	1.5	1.5	0.6	0.71–7.09	2.42 ± 0.08
								Global fit: k(295 K) = 2.50 ± 0.01
270	50	31.6	H_2O_2	1.6	1.9	7.0	0.43–2.15	2.22 ± 0.10
270	100	11.7	H_2O_2	1.9	1.7	7.2	0.46–2.94	2.19 ± 0.05

(Continues)

TABLE 1 (Continued)

T (K)	P (Torr)	v (cm s^{-1})	OH radical source	[Source] (10^{14} molecule cm^{-3})	Photolysis laser Fluence (mJ cm^{-2} pulse^{-1})	[OH]$_0$ (10^{10} molecule cm^{-3})	[L_4] (10^{14} molecule cm^{-3})	k(T)[a] (10^{-12} cm^{-3} molecule^{-1} s^{-1})
270	200	5.9	H_2O_2	1.5	1.8	6.2	1.36–2.94	2.26 ± 0.07
270	200	5.9	H_2O_2	1.4	1.6	5.1	0.35–3.34	2.19 ± 0.04
270	50	23.8	H_2O_2	1.5	1.6	5.4	0.38–3.75	2.25 ± 0.04
								Global fit: k(270 K) = 2.22 ± 0.01

[a]Quoted uncertainties are the 2σ precision from the least-square fit, global fit values were derived from linear least-squares fit to all data at that temperature.
[b]3.42×10^{16} molecule cm^{-3} O_2 added to the gas mixture.

TABLE 2 Summary of the experimental conditions and rate coefficients, k_2(T), obtained in this work for the OH + dodecamethylpentasiloxane (L_5) reaction.

T (K)	P (Torr)	v (cm s^{-1})	OH radical source	[Source] (10^{14} molecule cm^{-3})	Photolysis laser Fluence (mJ cm^{-2} pulse^{-1})	[OH]$_0$ (10^{10} molecule cm^{-3})	[L_5] (10^{14} molecule cm^{-3})	k(T)[a] (10^{-12} cm^{-3} molecule^{-1} s^{-1})
370	49	33.36	H_2O_2	2.0	1.9	8.5	0.35–1.24	4.88 ± 0.14
370	100	16.74	H_2O_2	1.5	1.8	6.0	0.26–1.49	4.71 ± 0.10
370	49	33.31	H_2O_2	1.4	1.8	5.7	0.16–1.22	4.90 ± 0.22
370	100	16.01	H_2O_2	1.3	1.3	3.8	0.22–1.60	5.06 ± 0.31
370	201	8.09	H_2O_2	1.1	1.5	3.9	0.19–1.52	4.66 ± 0.13
								Global fit: k(370 K) = 4.83 ± 0.07
340	100	15.37	H_2O_2	1.3	2.1	6.3	0.23–1.33	4.13 ± 0.18
340	49	30.22	H_2O_2	1.5	1.8	6.1	0.16–1.30	4.11 ± 0.12
340	100	15.04	H_2O_2	1.6	1.5	5.3	0.23–1.45	4.37 ± 0.19[b]
340	100	14.93	H_2O_2	1.7	1.5	5.6	0.20–1.44	4.28 ± 0.11
340	200	7.52	H_2O_2	1.2	1.5	4.1	0.25–1.55	4.07 ± 0.07
								Global fit: k(340 K) = 4.19 ± 0.05
320	100	14.07	H_2O_2	1.4	1.6	5.2	0.19–1.78	3.74 ± 0.12
320	200	7.08	H_2O_2	1.3	0.5	1.6	0.34–1.83	3.53 ± 0.17
320	49	27.93	H_2O_2	1.5	1.4	4.5	0.18–1.33	3.77 ± 0.11
320	200	6.98	H_2O_2	0.9	2.0	4.0	0.19–1.51	3.67 ± 0.11
320	100	15.31	HNO_3	10.8	1.6	4.4	0.25–1.71	3.53 ± 0.03
320	200	7.87	HNO_3	5.3	1.7	2.2	0.20–1.48	3.65 ± 0.11
								Global fit: k(320 K) = 3.64 ± 0.04
295	100	13.06	H_2O_2	1.7	1.9	7.0	0.45–1.82	3.15 ± 0.13
294	100	12.93	H_2O_2	1.9	1.9	8.0	0.69–1.27	3.23 ± 0.14
295	49	26.16	H_2O_2	1.5	1.8	6.1	0.37–1.41	2.93 ± 0.15
295	49	24.66	H_2O_2	1.5	1.6	5.5	0.20–1.45	3.14 ± 0.09
295	200	6.37	H_2O_2	0.9	1.5	3.0	0.21–1.18	3.37 ± 0.11
297	100	12.99	H_2O_2	1.8	1.4	5.6	0.21–2.20	3.12 ± 0.07
								Global fit: k(295 K) = 3.12 ± 0.04

[a]Quoted uncertainties are the 2σ precision from the least-square fit, global fit values were derived from linear least-squares fit to all data at that temperature.
[b]3.06×10^{16} molecule cm^{-3} O_2 added to the gas mixture.

TABLE 3 Summary of the experimental conditions and rate coefficients, k_3(T), obtained in this work for the OH + decamethylcyclopentasiloxane (D_5) reaction.

T (K)	P (Torr)	v (cm s^{-1})	OH radical source	[Source] (10^{14} molecule cm^{-3})	Photolysis laser Fluence (mJ cm^{-2} $pulse^{-1}$)	$[OH]_0$ (10^{10} molecule cm^{-3})	$[D_5]$ (10^{14} molecule cm^{-3})	k(T)[a] (10^{-12} cm^{-3} $molecule^{-1}$ s^{-1})
370	100	16.2	H_2O_2	1.3	2.0	6.0	0.42–3.33	3.26 ± 0.13
370	50	32.4	HNO_3	17.7	2.2	9.7	0.44–3.00	3.29 ± 0.17
370	100	16.5	HNO_3	16.1	2.2	8.8	0.34–2.64	3.22 ± 0.09
								Global fit: k(370 K) = 3.26 ± 0.04
340	100	14.7	H_2O_2	1.4	1.3	4.2	0.50–3.19	2.80 ± 0.10
340	50	29.8	H_2O_2	1.8	1.3	5.1	0.46–3.38	2.91 ± 0.10
340	100	16.0	HNO_3	14.5	1.7	6.2	0.61–3.42	2.67 ± 0.07
								Global fit: k(340 K) = 2.80 ± 0.05
320	50	29.1	HNO_3	15.0	2.2	8.3	0.37–2.28	2.44 ± 0.12
320	49	28.3	H_2O_2	1.7	2.0	7.5	0.36–4.09	2.37 ± 0.07
320	100	14.1	H_2O_2	1.6	1.9	6.9	1.35–3.28	2.35 ± 0.11
320	200	7.3	HNO_3	7.8	2.0	4.0	0.58–2.98	2.40 ± 0.06
320	200	7.5	HNO_3	7.1	1.8	3.1	0.55–3.84	2.31 ± 0.04
								Global fit: k(320 K) = 2.36 ± 0.02
295	100	12.9	H_2O_2	1.5	1.2	4.2	0.41–3.82	2.04 ± 0.09
295	101	12.8	H_2O_2	1.6	1.2	4.3	0.51–2.21	2.04 ± 0.11[b]
295	50	25.8	H_2O_2	2.0	1.6	7.1	0.55–3.49	1.97 ± 0.05
295	200	5.7	H_2O_2	1.1	1.4	3.4	0.99–4.15	2.01 ± 0.07
								Global fit: k(295 K) = 2.02 ± 0.02
270	50	23.4	H_2O_2	1.2	1.8	4.9	0.26–3.18	1.70 ± 0.03
270	101	11.6	H_2O_2	1.7	1.6	6.2	0.54–3.37	1.71 ± 0.06
270	100	12.0	H_2O_2	1.8	1.9	7.6	0.85–3.37	1.68 ± 0.06
270	200	6.0	H_2O_2	1.9	2.0	8.3	1.03–3.46	1.67 ± 0.06
								Global fit: k(270 K) = 1.69 ± 0.01

[a]Quoted uncertainties are the 2σ precision from the least-square fit, global fit values were derived from linear least-squares fit to all data at that temperature.
[b]3.59×10^{16} molecule cm^{-3} O_2 added to the gas mixture.

and S5. The rate coefficient data is of similar quality to that shown in Figure 2 for the L_4 reaction. Both cyclic permethylsiloxane reactions showed no dependence on variations in the experimental conditions as outlined in Tables 3 and 4. The final derived rate coefficient at each temperature was obtained from a fit of the combined data obtained at each temperature.

The temperature-dependent rate coefficient results for Reactions 3 and 4 are summarized in Figures 5 and 6, respectively. Both reactions show a positive temperature dependence, while the D_5 reaction displays a very weak non-Arrhenius behavior that falls within our estimated uncertainty range. The fit results are given in Table 5.

3.4 | Comparison with previous D_5 and D_6 studies

There are several studies for the D_5 reaction available for comparison with the present results, including two temperature-dependent studies with data between 313 and 353 K. The literature data is included in Table 5 and Figure 5 for comparison with the present results. The earliest measurement was performed by Atkinson[27] who reported $k_3(297\ \text{K}) = (1.55 \pm 0.49) \times 10^{-12}$ cm^{-3} $molecule^{-1}$ s^{-1}, which is significantly less than our room temperature value. Note that Akinson reported rather large uncertainty in the reported value. The studies of Safron et al.[30] and Xiao et al.[29] have considerable scatter and we have included

TABLE 4 Summary of the experimental conditions and rate coefficients, k_4(T), obtained in this work for the OH + dodecamethylcyclohexasiloxane (D_6) reaction.

T (K)	P (Torr)	v (cm s^{-1})	OH radical source	[Source] (10^{14} molecule cm^{-3})	Photolysis laser Fluence (mJ cm^{-2} $pulse^{-1}$)	$[OH]_0$ (10^{10} molecule cm^{-3})	$[D_6]$ (10^{14} molecule cm^{-3})	k(T) [a] (10^{-12} cm^{-3} $molecule^{-1}$ s^{-1})
370	200	8.2	H_2O_2	1.5	1.3	4.4	0.160–0.417	5.05 ± 0.13
370	100	16.1	H_2O_2	1.5	1.2	3.9	0.057–0.559	4.85 ± 0.08
370	100	16.0	H_2O_2	1.2	1.3	3.4	0.098–0.972	4.32 ± 0.21
370	200	8.0	H_2O_2	1.0	1.1	2.5	0.202–0.874	4.52 ± 0.42
								Global fit: k(370 K) = 4.53 ± 0.11
340	100	14.8	H_2O_2	1.3	1.3	3.7	0.102–0.585	3.70 ± 0.12
340	200	7.4	H_2O_2	1.2	1.3	3.5	0.117–0.618	4.01 ± 0.06
340	101	8.5	H_2O_2	1.3	1.3	3.6	0.093–1.002	3.68 ± 0.21
340	100	14.8	H_2O_2	1.3	1.4	4.1	0.081–0.623	3.59 ± 0.22
340	200	7.3	H_2O_2	1.1	1.3	3.2	0.110–0.626	4.01 ± 0.26
340	100	14.7	H_2O_2	1.4	1.2	3.8	0.167–0.618	3.47 ± 0.15
								Global fit: k(340 K) = 3.74 ± 0.07
320	100	13.3	H_2O_2	1.4	1.4	4.3	0.112–0.627	3.51 ± 0.06
320	201	7.1	H_2O_2	1.3	1.2	3.5	0.090–0.568	3.09 ± 0.23
320	100	13.7	H_2O_2	1.5	1.1	3.9	0.211–0.663	3.19 ± 0.06
320	200	7.1	H_2O_2	1.4	1.1	3.5	0.127–0.672	3.47 ± 0.16
320	201	7.0	H_2O_2	1.3	1.2	3.2	0.110–0.678	3.22 ± 0.18
								Global fit: k(320 K) = 3.24 ± 0.07
296	100	12.9	H_2O_2	1.3	1.6	4.4	0.111–0.758	2.75 ± 0.13
297	200	6.4	H_2O_2	1.5	1.5	5.2	0.230–0.785	2.88 ± 0.37
297	100	13.0	H_2O_2	1.4	1.4	4.5	0.112–0.599	2.90 ± 0.25[b]
297	201	6.4	H_2O_2	0.9	1.3	2.8	0.124–0.718	2.81 ± 0.13
297	100	12.8	H_2O_2	1.5	1.2	4.0	0.176–0.559	2.77 ± 0.32
								Global fit: k(297 K) = 2.89 ± 0.05

[a]Quoted uncertainties are the 2σ precision from the least-square fit, global fit values were derived from linear least-squares fit to all data at that temperature.
[b]3.51×10^{16} molecule cm^{-3} O_2 added to the gas mixture.

average values at each of the temperatures in their studies in Figure 5. The results from these studies are systematically greater than the present results, although they fall within the uncertainties shown in Figure 5. Although the Safron et al. and Xiao et al. studies report a positive temperature dependence for k_3(T), with E/R values of 517 and 402 K, respectively, these parameters are not statistically significant given the scatter in the experimental data. Note that E/R uncertainties were not reported in their work. In a recent study, Alton and Browne[26] reported k_3(297 K) = (2.1 ± 0.1) × 10^{-12} cm^{-3} $molecule^{-1}$ s^{-1}, which is in good agreement with our room temperature value.

Safron et al.[30] is the only previous study of the D_6 reaction available in the literature. Their average rate coefficient data at their measurement temperatures are included in Figure 6. Their reported Arrhenius expression is given in Table 5. The scatter in their kinetic data is substantial and the reported positive temperature dependence, E/R = 517 K, is not statistically significant. Their average results agree with the present results to within ~20%.

3.5 | Reactivity trends

In this section, we summarize the results obtained in this work and discuss trends in the permethylsiloxane reactivity. Alton and Browne[26] provided an SAR for permethylsiloxanes, which has been updated here to include rate coefficient temperature dependence parameterization.

INTERNATIONAL JOURNAL OF CHEMICAL KINETICS WILEY

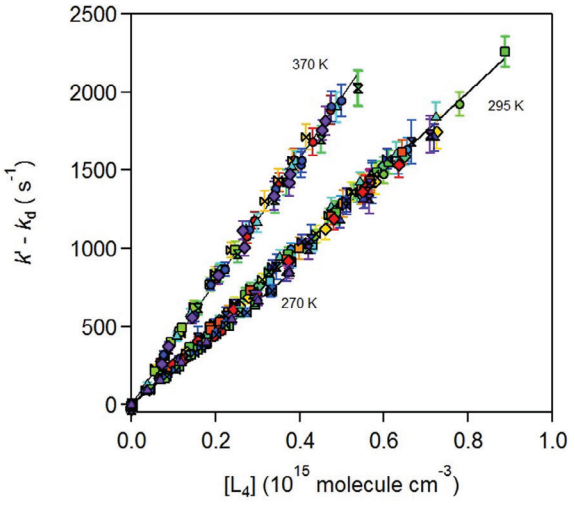

FIGURE 2 Pseudo first-order rate coefficient data for the OH + decamethyltetrasiloxane ($(CH_3)_3SiO[Si(CH_3)_2O]_2Si(CH_3)_3$, L_4) reaction obtained at 295 K and the temperature extremes of this study, 270 and 370 K. The data obtained at 320 and 340 K is not included for clarity reasons. The error bars are the 2σ precision of the measurement. The different symbols and colors represent results from independent experiments. The lines are linear least-squares fits of all the data at each temperature (see Table 1).

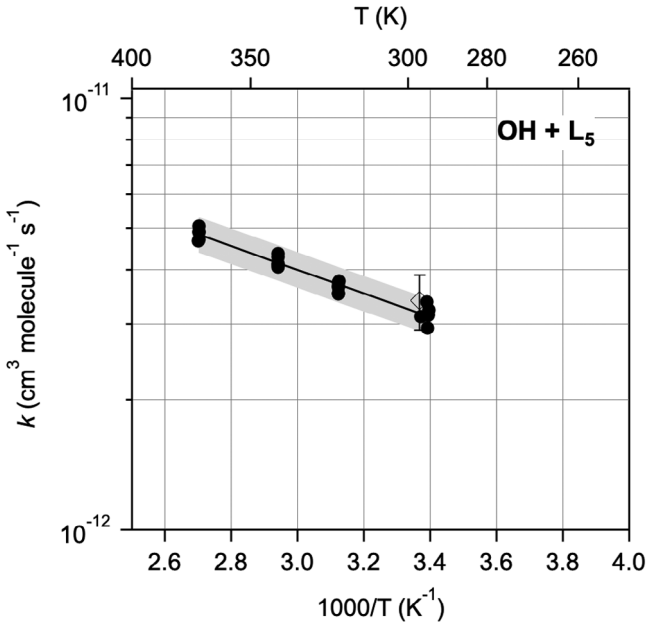

FIGURE 4 Rate coefficient data for the OH + dodecamethylpentasiloxane ($(CH_3)_3SiO[Si(CH_3)_2O]_3Si(CH_3)_3$, L_5) reaction obtained in this study using the absolute pulsed laser photolysis-laser induced fluorescence (PLP–LIF) technique (●), see Table 2. The extremes of the gray-shaded region represent the range of the estimated absolute uncertainty, ±10%. The lines are least-squares fits and the parameters are given in Table 5. Literature data from Alton and Browne[26] (◇) is included for comparison (see Table 5).

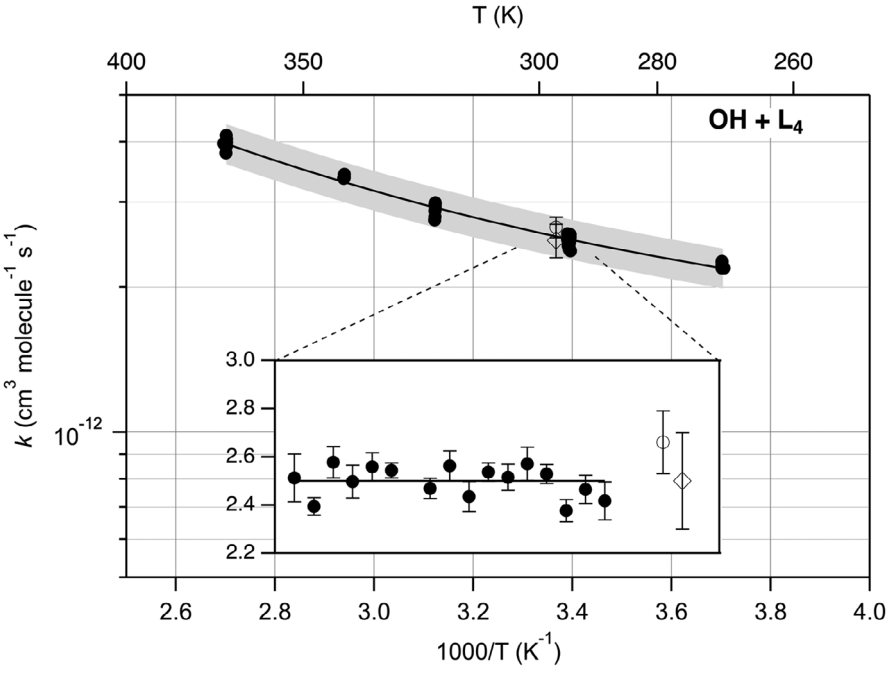

FIGURE 3 Rate coefficient data for the OH + decamethyltetrasiloxane ($(CH_3)_3SiO[Si(CH_3)_2O]_2Si(CH_3)_3$, L_4) reaction obtained in this study using the absolute pulsed laser photolysis-laser induced fluorescence (PLP–LIF) technique (●), see Table 1. The lines are least-squares fits and the parameters are given in Table 5. The extremes of the gray-shaded region represent the range of the estimated absolute uncertainty, ±10%. Literature data from Markgraf and Wells[28] (○) and Alton and Browne[26] (◇) are included for comparison and their results are also included in Table 5.

TABLE 5 Summary of OH + permethylsiloxane rate coefficients and parameterizations obtained in this work and literature values.

Permethylsiloxane	T (K)	k(295 K)[a] (10^{-12} cm^{-3} molecule^{-1} s^{-1})	k(T) (cm^{-3} molecule^{-1} s^{-1})	Method[b]	Reference
$(CH_3)_3SiO[Si(CH_3)_2O]_2Si(CH_3)_3$, L_4	270–370	2.50 ± 0.18	1.707×10^{-13} (T/298)$^{4.45}$ exp[807/T]	PLP–LIF	This work
	297 ± 3	2.5 ± 0.2	–	RR	Alton and Browne (2020)[26]
	297 ± 3	2.66 ± 0.13	–	RR[c,d]	Markgraf and Wells (1997)[28]
$(CH_3)_3SiO[Si(CH_3)_2O]_3Si(CH_3)_3$, L_5	295–370	3.12 ± 0.32	$(2.65 \pm 0.02) \times 10^{-11}$ exp[−(630 ± 60)/T]	PLP–LIF	This work
	297 ± 3	3.4 ± 0.5	–	RR	Alton and Browne (2020)[26]
$[-Si(CH_3)_2O-]_5$, D_5	270–370	2.02 ± 0.12	8.97×10^{-13} (T/298)$^{2.90}$ exp[248/T]	PLP–LIF	This work
	297 ± 3	2.1 ± 0.1	–	RR	Alton and Browne (2020)[26]
	313–353	–	1.1×10^{-11} exp(−517/T)	RR[d]	Safron et al. (2015)[30]
	313–353	–	9.46×10^{-12} exp(−402/T)	RR[e]	Xiao et al. (2015)[29]
	297 ± 2	1.45 ± 0.49	–	RR[d]	Atkinson (1991)[27]
$[-Si(CH_3)_2O-]_6$, D_6	297–370	2.89 ± 0.16	$(3.13 \pm 0.05) \times 10^{-11}$ exp[−(717 ± 119)/T]	PLP–LIF	This work
	313–353	–	1.7×10^{-11} exp(−517/T)	RR[d]	Safron et al. (2015)[30]

[a]Uncertainties from this work are estimated 2σ absolute values, uncertainties for literature values are their reported values.
[b]PLP-LIF: pulsed laser photolysis–laser induced fluorescence technique; RR: relative rate technique.
[c]Rate coefficient calculated using the reported k/k_{Ref} and k(OH + n-hexane) = 5.20×10^{-12} cm^{-3} molecule^{-1} s^{-1} at 298 K.[46]
[d]Rate coefficient calculated using k(OH + cyclohexane) = 6.97×10^{-12} cm^{-3} molecule^{-1} s^{-1} at 298 K.[46] The Atkinson value has been decreased by 7% to reflect this reference value.
[e]OH + 2,2,4-trimethylpentane (TMP) was the reference reaction, however, rate coefficient ratios and reference rate coefficient were not reported.

Figure 7 and Table 5 summarize the permethylsiloxane rate coefficient data from this study for the temperature dependent OH radical rate coefficient with L_4, L_5, D_5, and D_6 permethylsiloxanes.

The rate coefficients show a systematic increase with the number of methyl groups, with the linear compounds having a greater reactivity than the cyclic compounds with an equivalent number of methyl groups. The temperature dependent rate coefficients for the OH + permethylsiloxane reactions are consistent with reactions that proceed via a H-atom abstraction mechanism.

A comparison of the OH reactivity of permethylsiloxanes with analogous hydrocarbons with similar molecular structures shows some significant differences between the carbon and silicon-based compounds. For example, di-*tert*-butyl ether [DTBE, $(CH_3)_3COC(CH_3)_3$] is analogous to hexamethyldisiloxane (L_2, $(CH_3)_3SiOSi(CH_3)_3$). The reaction of OH with di-tert-butyl ether has been reported at 296 K by Nielsen et al.[38] and Langer et al.[39] with an average value of k(296 K) = 3.85×10^{-12} cm^{-3} molecule^{-1} s^{-1}. By comparison, the OH rate coefficient for hexamethyldisiloxane is almost three times less than that of DTBE. The difference in OH reactivity may be explained by the higher electronegativity of carbon versus Si, increasing the negative inductive effect in the C–H bonds of the $-CH_3$ group.

Alton and Browne[26] have applied a SAR analysis to their OH + permethylsiloxane 298 K rate coefficient data using methods analogous to that developed in the seminal work of Atkinson[40] and Kwok and Atkinson.[41] The reaction pathway for the OH radical reaction is H-atom abstraction from $-CH_3$ functionalities with differences in the surrounding environment accounted for by enhancement factors F(X), where X represents the surrounding environment. The total reaction rate coefficient is represented as the sum of the reaction at all the available reaction sites. They used a F(–Si(CH$_3$)$_2$OR) substituent factor of 1.9 for α-Si atom in the terminal position of a linear permethylsiloxane and a F(–SiCH$_3$(OR)$_2$) of 1.5 for a α-Si atom in the center of a linear VMS or in a cyclic permethylsiloxane. The parameterization reproduces their experimental data to within ~15%, on average, with small

INTERNATIONAL JOURNAL OF CHEMICAL KINETICS WILEY

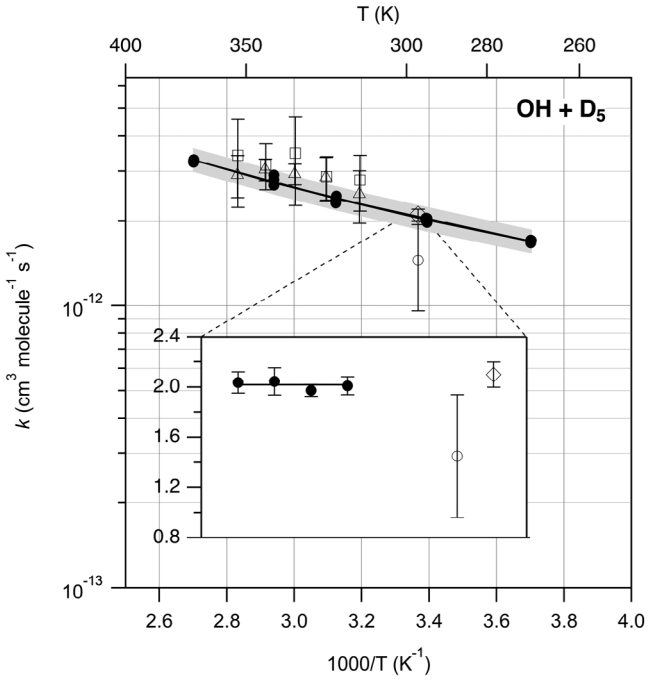

FIGURE 5 Rate coefficient data for the OH + decamethylcyclopentasiloxane ($[-Si(CH_3)_2O-]_5$, D_5) reaction obtained in this study using the absolute pulsed laser photolysis-laser induced fluorescence (PLP–LIF) technique (●), see Table 5. The extremes of the gray-shaded region represent the range of the estimated absolute uncertainty, ±10%. The solid lines are least-squares fits (see Table 3). Literature data from Safron et al.[30] (□), Xiao et al.[29] (△), Atkinson[27] (○), and Alton and Browne[26] (◇) are included for comparison (see Table 5). Data from Safron et al.[30] and Xiao et al.[29] have been averaged at each temperature and the error bars are the 2σ standard deviation of the average.

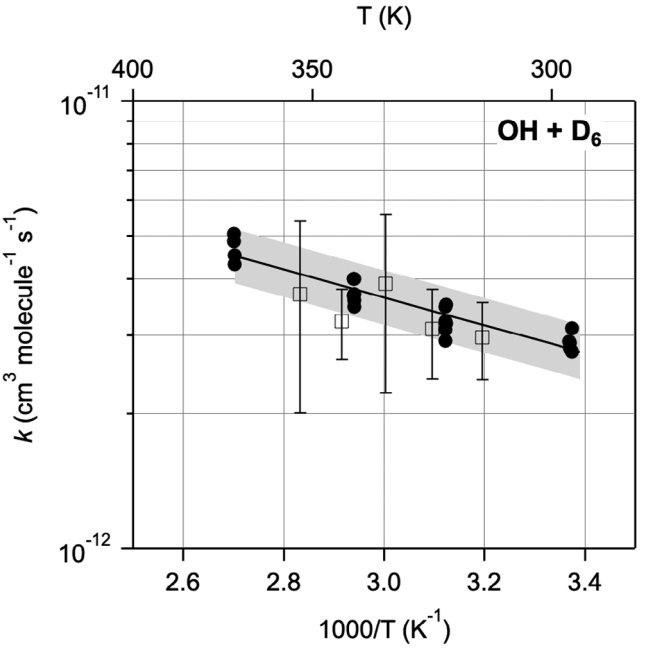

FIGURE 6 Rate coefficient data for the OH + dodecamethylcyclohexasiloxane ($[-Si(CH_3)_2O-]_6$, D_6) reaction obtained in this study using the absolute pulsed laser photolysis-laser induced fluorescence (PLP–LIF) technique (●), see Table 4. The extremes of the gray-shaded region represent the range of the estimated absolute uncertainty, ±15%. The solid line is the least-squares fit and the parameters are given in Table 5. Literature data from Safron et al.[30] (□) was averaged at each temperature where error bars are the 2σ standard deviation of the average. Their results are given in Table 5.

molecules being under-predicted and the larger molecules over-predicted.

A SAR analysis of the present temperature-dependent rate coefficient data and that from our previous study[31] of L_2, L_3, D_3, and D_4 was performed. In our analysis, $F(-OSi(CH_3)_3)$ and $F(-OSi(CH_3)_2-)$ substituent enhancement factors are taken to be equal, $F(X)$. For the cyclic compounds, a ring-strain factor, F_{ring}, was applied as previously used by Atkinson[40] for cyclo-alkanes, which showed that the presence of ring-strain leads to a lower OH rate coefficient.[42]

$F(X)$ was obtained by fitting the linear permethylsiloxane $k(T)$ data using the expression:

$$k(T) = F(X) \times N_{CH3} \times k_{prim}(T) \quad (10)$$

where N_{CH3} is the number of methyl groups and $k_{prim}(T) = 4.49 \times 10^{-18}\ T^2\ \exp(-320/T)$.[41] The temperature dependence of the substituent factor was formulated as $F(X) = \exp(E_X/T)$.[41] The temperature dependent expression for $F(X)$ was found to be $\exp(155/T)$, where $F(X) = 1.68$ at 298 K. The SAR analysis for the linear permethylsiloxanes reproduced the experimental data to within ~10%–15% at all temperatures, which is within the measurement accuracy, see Figure 8. There is a slight systematic discrepancy at the lowest temperatures primarily because the temperature dependence formulation used does not account for the observed weak non-Arrhenius behavior. However, a more detailed parameterization is not warranted. Overall, the SAR parametrization of the linear permethylsiloxanes kinetic data is excellent.

For the cyclic permethylsiloxanes, a multiplicative ring-strain factor was added to the parameterization, while keeping the parameterization derived for the linear compounds. The SAR calculated and experimentally measured rate coefficients are shown in Figure 8. Ring-strain factors of 0.67, 0.67, 0.83, and 1.0 were applied to D_3, D_4, D_5, and D_6, respectively. That is, the smallest ring compounds showed the greatest ring-strain, while D_6 showed no ring-strain. This is consistent with the increased entropy (flexibility) with increasing ring size. There was no observable temperature dependence to the ring-strain factor. The SAR parameterization of the cyclic permethylsiloxanes is

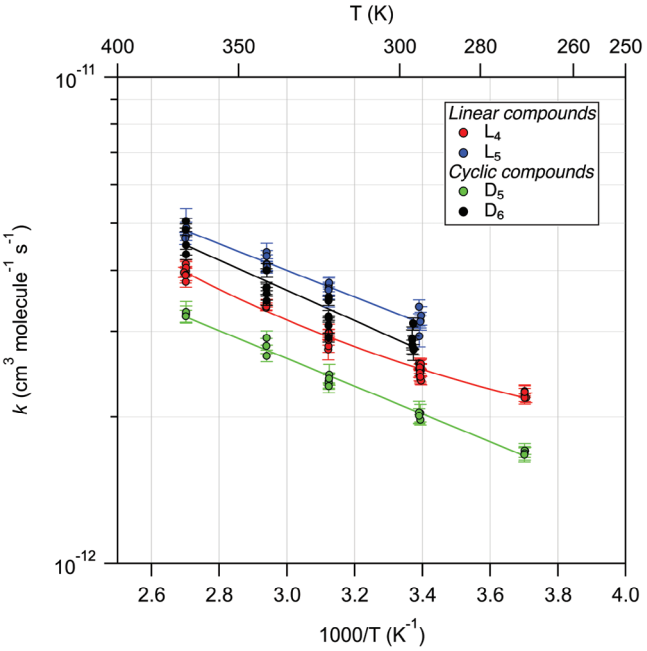

FIGURE 7 Summary of the rate coefficients obtained in this study for the reaction of OH with $(CH_3)_3SiO[Si(CH_3)_2O]_2Si(CH_3)_3$ (L_4), $(CH_3)_3SiO[Si(CH_3)_2O]_3Si(CH_3)_3$ (L_5), $[-Si(CH_3)_2O-]_5$ (D_5), and $[-Si(CH_3)_2O-]_6$ (D_6) (see Tables 1–4). The lines are least-squares fits to the data and the fit parameters are given in Table 5.

excellent and reproduces the experimental data to better than the actual measurement accuracy.

4 | CONCLUSIONS

In this study, rate coefficients for the gas-phase OH radical reaction with linear and cyclic low-volatility permethylsiloxanes (L_4, L_5, D_5, and D_6) were measured over the temperature range 270–370 K using absolute pulsed laser photolysis—laser induced fluorescence technique. Over this temperature range, the reactions display a positive temperature dependence consistent with a H-abstraction reaction mechanism. The L_4 and D_5 reaction rate coefficients displayed a weak non-Arrhenius behavior described well by a $A(T/298)^n\exp(E/RT)$ expression.

For a globally averaged OH radical concentration of 1×10^6 molecule cm^{-3}, the atmospheric lifetimes for the L_4, L_5, D_5, and D_6 permethylsiloxanes are estimated to be 5.2, 4.4, 6.8, and 5.2 days, respectively. These permethylsiloxanes are, therefore, considered to be very-short lived substances (VSLs) that would impact local and regional tropospheric chemistry and air quality. The atmospheric degradation mechanism of permethylsiloxanes and the formation of stable end-products that may contribute to the formation of secondary aerosol remains a topic of current theoretical[29,43–45] and experimental interest.[20,26]

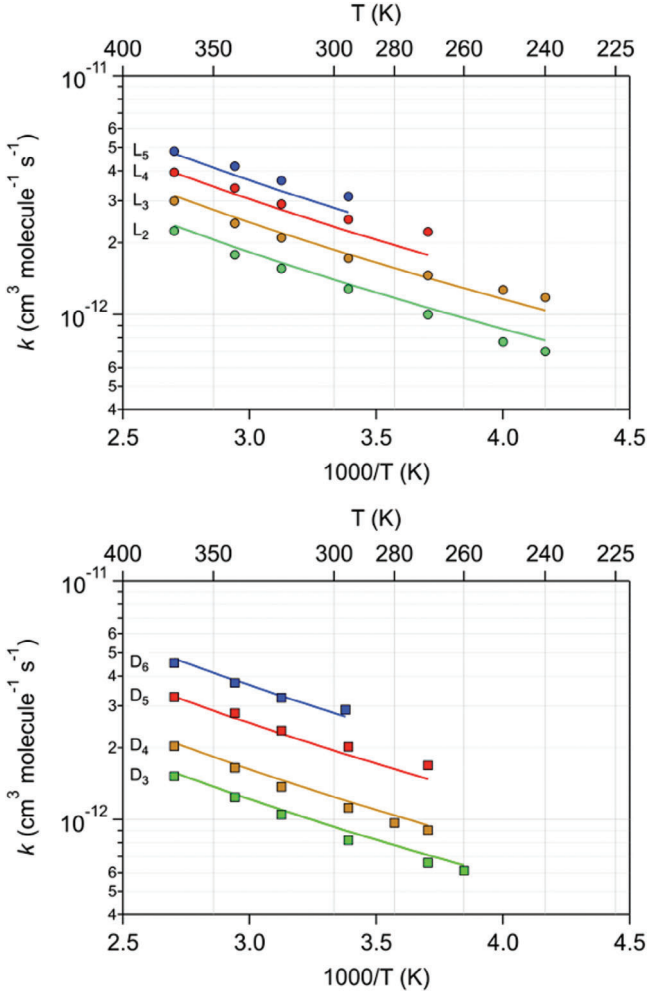

FIGURE 8 Structure activity relationship (SAR) analysis of linear (upper panel) and cyclic (lower) OH + permethylsiloxane reaction rate coefficient data measured in this work and from our previous study.[31] The data points are the measured rate coefficients and the lines are the SAR parameterization (see text).

DATA AVAILABILITY STATEMENT

The data that supports the findings of this study are available in the supplementary material of this article.

ORCID

François Bernard https://orcid.org/0000-0002-6116-3167
James B. Burkholder https://orcid.org/0000-0001-9532-6246

REFERENCES

1. McDonald BC, de Gouw JA, Gilman JB, et al. Volatile chemical products emerging as largest petrochemical source of urban organic emissions. *Science*. 2018;359:760-764.
2. Coggon MM, McDonald BC, Vlasenko A, et al. Diurnal variability and emission pattern of decamethylcyclopentasiloxane (D_5) from the application of personal care products in two North American cities. *Environ Sci Technol*. 2018;52:5610-5618.

3. Buser AM, Kierkegaard A, Bogdal C, MacLeod M, Scheringer M, Hungerbühler K. Concentrations in ambient air and emissions of cyclic volatile methylsiloxanes in Zurich, Switzerland. *Environ Sci Technol*. 2013;47:7045-7051.
4. Buser AM, Bogdal C, MacLeod M, Scheringer M. Emissions of decamethylcyclopentasiloxane from Chicago. *Chemosphere*. 2014;107:473-475.
5. Gkatzelis GI, Coggon MM, McDonald BC, et al. Identifying volatile chemical product tracer compounds in US cities. *Environ Sci Tech*. 2021;55:188-199.
6. Tang X, Misztal PK, Nazaroff WW, Goldstein AH. Siloxanes are the most abundant volatile organic compound emitted from engineering students in a classroom. *Environ Sci Tech Lett*. 2015;2:303-307.
7. Pieri F, Katsoyiannis A, Martellini T, Hughes D, Jones KC, Cincinelli A. Occurrence of linear and cyclic volatile methyl siloxanes in indoor air samples (UK and Italy) and their isotopic characterization. *Environ Inter*. 2013;59:363-371.
8. Li Q, Lv X, Hu JC, Wang X, Ma JM. Typical indoor concentrations and mass flow of cyclic volatile methylsiloxanes (cVMSs) in Dalian, China. *Chemosphere*. 2020;248:126020.
9. Katz EF, Lunderberg DM, Brown WL, et al. Large emissions of low-volatility siloxanes during residential oven use. *Environ Sci Technol Lett*. 2021;8:519-524.
10. Molinier B, Arata C, Katz EF, et al. Volatile methyl siloxanes and other organosilicon compounds in residential air. *Environ Sci Technol*. 2022;56:15427-15436.
11. Genualdi S, Harner T, Cheng Y, et al. Global distribution of linear and cyclic volatile methyl siloxanes in air. *Environ Sci Technol*. 2011;45:3349-3354.
12. Krogseth IS, Kierkegaard A, McLachlan MS, Breivik K, Hansen KM, Schlabach M. Occurrence and seasonality of cyclic volatile methyl siloxanes in Arctic air. *Environ Sci Technol*. 2013;47:502-509.
13. Wang X, Schuster J, Jones KC, Gong P. Occurrence and spatial distribution of neutral perfluoroalkyl substances and cyclic volatile methylsiloxanes in the atmosphere of the Tibetan Plateau. *Atmos Chem Phys*. 2018;18:8745-8755.
14. Kierkegaard A, McLachlan MS. Determination of linear and cyclic volatile methylsiloxanes in air at a regional background site in Sweden. *Atmos Environ*. 2013;80:322-329.
15. Janechek NJ, Hansen KM, Stanier CO. Comprehensive atmospheric modeling of reactive cyclic siloxanes and their oxidation products. *Atmos Chem Phys*. 2017;17:8357-8370.
16. Whelan MJ, Kim J. Application of multimedia models for understanding the environmental behavior of volatile methylsiloxanes: fate, transport, and bioaccumulation. *Int Environ Assess Manag*. 2022;18:599-621.
17. Xu S, Wania F. Chemical fate, latitudinal distribution and long-range transport of cyclic volatile methylsiloxanes in the global environment: a modeling assessment. *Chemosphere*. 2013;93:835-843.
18. Bzdek BR, Horan AJ, Pennington MR, et al. Silicon is a frequent component of atmospheric nanoparticles. *Environ Sci Technol*. 2014;48:11137-11145.
19. Pennington MR, Klems JP, Bzdek BR, Johnston MV. Nanoparticle chemical composition and diurnal dependence at the Calnex Los Angeles ground site. *J Geophys Res*. 2012;117:D00V10.
20. Wu Y, Johnston MV. Aerosol formation from OH oxidation of the volatile cyclic methyl siloxane (cVMS) decamethylcyclopentasiloxane. *Environ Sci Technol*. 2017;51:4445–4451.
21. Chandramouli B, Kamens RM. The photochemical formation and gas-particle partitioning of oxidation products of decamethyl cyclopentasiloxane and decamethyl tetrasiloxane in the atmosphere. *Atmos Environ*. 2001;35:87-95.
22. Charan SM, Huang Y, Buenconsejo RS, Li Q, Cocker DR, Seinfeld JH. Secondary organic aerosol formation from the oxidation of decamethylcyclopentasiloxane at atmospherically relevant OH concentrations. *Atmos Chem Phys*. 2022;22:917-928.
23. Janechek NJ, Marek RF, Bryngelson N, et al. Physical properties of secondary photochemical aerosol from OH oxidation of a cyclic siloxane. *Atmos Chem Phys*. 2019;19:1649-1664.
24. Avery AM, Alton MW, Canagaratna MR, et al. Comparison of the yield and chemical composition of secondary organic aerosol generated from the OH and Cl oxidation of decamethylcyclopentasiloxane. *ACS Earth Space Chem*. 2023;7:218-229.
25. Zhang Y, Shen M, Tian Y, Zeng G. Cyclic volatile methylsiloxanes in sediment, soil, and surface water from Dongting Lake, China. *J Soils Sed*. 2018;18:2063-2071.
26. Alton MW, Browne EC. Atmospheric chemistry of volatile methyl siloxanes: kinetics and products of oxidation by OH radicals and Cl atom. *Environ Sci Technol*. 2020;54:5992-5999.
27. Atkinson R. Kinetics of the gas-phase reactions of a series of organosilicon compounds with OH and NO_3 radicals and O_3 at 297 ± 2 K. *Environ Sci Technol*. 1991;25:863-866.
28. Markgraf SJ, Wells JR. The hydroxyl radical reaction rate constants and atmospheric reaction products of three siloxanes. *Inter J Chem Kinet*. 1997;29:445-451.
29. Xiao R, Zammit I, Wei Z, Hu W-P, MacLeod M, Spinney R. Kinetics and mechanism of the oxidation of cyclic methylsiloxanes by hydroxyl radical in the gas phase: an experimental and theoretical study. *Environ Sci Technol*. 2015;49:13322-13330.
30. Safron A, Strandell M, Kierkegaard A, Macleod M. Rate constants and activation energies for gas-phase reactions of three cyclic volatile methyl siloxanes with the hydroxyl radical. *Inter J Chem Kinet*. 2015;47:420-428.
31. Bernard F, Papanastasiou DK, Papadimitriou VC, Burkholder JB. Temperature dependent rate coefficients for the gas-phase reaction of the OH radical with linear (L_2, L_3) and cyclic (D_3, D_4) permethylsiloxanes. *J Phys Chem A*. 2018;122:4252-4264.
32. Vaghjiani GL, Ravishankara AR. Kinetics and mechanism of hydroxyl radical reaction with methyl hydroperoxide. *J Phys Chem*. 1989;93:1948-1959.
33. McGillen MR, Baasandorj M, Burkholder JB. Gas-phase rate coefficients for the OH + *n*-, *i*-, *s*-, and t-butanol reactions measured between 220 and 380 K: non-Arrhenius behavior and site-specific reactivity. *J Phys Chem A*. 2013;117:4636-4656.
34. Burkholder JB, Sander SP, Abbatt J, et al. Chemical kinetics and photochemical data for use in atmospheric studies, evaluation No. 19. JPL Publication 19-5, Jet Propulsion Laboratory, Pasadena, 2020. 2019. http://jpldataeval.jpl.nasa.gov
35. Baasandorj M, Papanastasiou DK, Talukdar RK, Hasson AS, Burkholder JB. $(CH_3)_3COOH$ (*tert*-butyl hydroperoxide): OH reaction rate coefficients between 206 and 375 K and the OH photolysis quantum yield at 248 nm. *Phys Chem Chem Phys*. 2010;12:12101-12111.

36. Bernard F, Papanastasiou DK, Papadimitriou VC, Burkholder JB. Infrared absorption spectra of linear (L_2-L_5) and cyclic (D_3-D_6) permethylsiloxanes. *J Quant Spectros Rad Trans*. 2017;202:247-254.
37. Davis ME, Burkholder JB. Rate coefficients for the gas-phase reaction of OH with (Z)-3-hexen-1-ol, 1-penten-3-ol, (E)-2-penten-1-ol, and (E)-2-hexen-1-ol between 243 and 404 K. *Atmos Chem Phys*. 2011;11:3347-3358.
38. Nielsen OJ, Sehested J, Langer S, Ljungström E, Wängberg I. UV absorption spectra and kinetics for alkyl and alkyl peroxy radicals originating from di-tert-butyl ether. *Chem Phys Lett*. 1995;238:359-364.
39. Langer S, Ljungström E, Wängberg I, Wallington TJ, Hurley MD, Nielsen OJ. Atmospheric chemistry of di-tert-butyl ether: rates and products of the reactions with chlorine atoms, hydroxyl radicals, and nitrate radicals. *Intern J Chem Kinet*. 1996;28:299-306.
40. Atkinson R. Kinetics and mechanisms of the gas-phase reactions of the hydroxyl radical with organic compounds under atmospheric conditions. *Chem Rev*. 1986;86:69-201.
41. Kwok ESC, Atkinson R. Estimation of hydroxyl radical reaction rate constants for gas-phase organic compounds using a structure-reactivity relationship: an update. *Atmos Environ*. 1995;29:1685-1695.
42. Atkinson R, Aschmann SM, Carter WPL. Rate constants for the gas-phase reactions of OH radicals with a series of bi- and tricycloalkanes at 299 ± 2 K: effects of ring strain. *Int J Chem Kinet*. 1983;15:37-50.
43. Ren ZH, da Silva G. Auto-oxidation of a volatile silicon compound: a theoretical study of the atmospheric chemistry of tetramethylsilane. *J Phys Chem A*. 2020;124:6544-6551.
44. Alton MW, Johnson VL, Sharma S, Browne EC. Volatile methyl siloxane atmospheric oxidation mechanism from a theoretical perspective—how is the diloxanol formed? *J Phys Chem A*. 2023;127:10233-10242.
45. Fu Z, Xie H-B, Elm J, Guo X, Fu Z, Chen J. Formation of low-volatile products and unexpected high formaldehyde yield from the atmospheric oxidation of methylsiloxanes. *Environ Sci Technol*. 2020;54:7136-7145.
46. Atkinson R. Kinetics of the gas-phase reactions of OH radicals with alkanes and cycloalkanes. *Atmos Chem Phys*. 2003;3:2233-2307.

SUPPORTING INFORMATION

Additional supporting information can be found online in the Supporting Information section at the end of this article.

How to cite this article: Bernard F, Burkholder JB. Rate coefficients for the gas-phase reaction of OH radicals with the L_4, L_5, D_5, and D_6 permethylsiloxanes. *Int J Chem Kinet*. 2025;57:199–212. https://doi.org/10.1002/kin.21769